16th World Conference on Earthquake, 16WCEE 2017
Santiago Chile, January 9th to 13th 2017
Paper N° 2263 (Abstract ID)
Registration Code: S-Y1464102561

Influence of Modelling on the Response of Asymmetric Buildings

M. Bosco[(1)], G.A.F Ferrara[(2)], A. Ghersi[(3)], E.M. Marino[(4)], P.P. Rossi[(5)]

[(1)] *Research Assistant, University of Catania, mbosco@dica.unict.it*
[(2)] *Doctor researcher, University of Catania, gferrara@dica.unict.it*
[(3)] *Full Professor, University of Catania, aghersi@dica.unict.it*
[(4)] *Assistant Professor, University of Catania, emarino@dica.unict.it*
[(5)] *Associate Professor, University of Catania, prossi@dica.unict.it*

Abstract

In several earthquake-prone countries, many buildings have not been designed by seismic regulations and others have been constructed according to old seismic codes. Effective methods of analysis are expected to be available to evaluate the seismic performance of these buildings and to validate interventions of structural rehabilitation. The linear method of analysis, used for the design of new buildings, is however not suitable for this purpose because the plastic collapse mechanism of existing structures, and thus the behavior factor, is not known a priori. Consequently, this method of analysis does not provide a reliable prediction of the response of existing structures. Instead, the nonlinear dynamic analysis and the nonlinear static analysis consider the inelastic deformation of structural members and can predict the seismic response of existing buildings effectively. However, the response provided by these nonlinear methods of analysis can be strongly affected by the accuracy of modelling. Idealized beam and column models for nonlinear analysis vary greatly in terms of complexity and computational efficiency. Available finite element models for the nonlinear material response of beam–column members have fallen into two categories: concentrated plasticity and distributed plasticity.

In this paper, the influence of modelling in the evaluation of the lateral torsional coupling of asymmetric buildings is investigated. In particular, four models are compared. In all the models, force Beam-Column elements are used to simulate the response of beams and columns. Further, in the first model considered, fiber cross-sections are assigned within the hinge region. This model is able to simulate the behavior of columns subjected to axial forces and biaxial bending. Instead, in the other models, two independent moment–curvature relationships are assigned within the hinge region to simulate the nonlinear behavior along two orthogonal axes of the cross-section. The adopted moment-curvature relationship is obtained starting from the moment-curvature analysis of the fiber cross-section subjected to the axial force produced by gravity loads. In particular, the moment-curvature relationship assumed in the nonlinear analysis is obtained by the previous curve by multi- or bi-linearization within the relevant range of curvatures.

The four considered models are adopted to predict the nonlinear (dynamic and static) response of an asymmetric building designed in a previous research. All the analyses are performed by the OpenSees Computer program.

Keywords: nonlinear dynamic analysis, nonlinear static analysis, fiber cross-sections, moment-curvature relationships

1. Introduction

Performance-based seismic design and assessment require accurate nonlinear finite element models that can capture the full range of structural response associated with various performance targets. Idealized beam and column models for nonlinear structural analysis vary greatly in terms of complexity and computational efficiency. Concentrated plasticity models were developed at first. In these models, the nonlinear behavior of a beam–column member is lumped into rotational springs at the ends of a linear-elastic element. The two-component model [1] and the one component model [2] are the most common approaches for concentrated plasticity beam–column elements. The main disadvantage of concentrated plasticity models is that they separate axial-moment interaction from the element behavior. Consequently, the moment-rotation relationship of the ending spring has to be calibrated based on the expected axial load and moment gradient along the member.

More recently, distributed plasticity finite elements have been used to model the beam-columns elements. These elements are based on either the displacement- or force-based formulation. Force-based beam-column elements have been shown to be advantageous over displacement-based elements for material nonlinear frame analysis by avoiding the discretization of structural members into numerous finite elements, thereby reducing the number of model degrees of freedom. The main advantages of distributed plasticity finite elements are: 1) plastic hinges may form at any location, 2) the interaction between axial force – and biaxial bending moment is automatically taken into account by discretizing the cross-section into fibers. However, the strain-softening behavior of concrete can cause localization in beam–column elements, particularly in the simulation of reinforced concrete columns that carry high gravity loads [3].

To overcome this limit, force-based finite-length plastic hinge beam-column elements have been recently proposed. These elements are composed of two discrete plastic hinges and a linear elastic region. Generally, fiber cross-sections are assigned within the hinge region. However, to limit the computational effort and in keeping with the concentrated plasticity models, two independent moment–curvature relationships can be assigned within the hinge region to simulate the nonlinear behavior along two orthogonal axes of the cross-section. When independent moment–curvature relationships are assigned, the interaction between axial forces and bending moments are neglected. At the same time, the reduction of the strength capacity of columns due to bi-axial bending is neglected.

In this paper, the effect of the modelling on the prediction of the nonlinear (dynamic and static) response for multi-story asymmetric structure is studied. To this end, finite-length plastic hinge beam-column elements are adopted to model the members of an asymmetric building designed in a previous research. Either fiber cross-sections or moment-curvature relationships are assigned within the plastic hinge length.

2. Methodology

As a general consideration, three features are expected to be responsible for the difference in the response predicted by the models: 1) the interaction between axial force and bending moment; 2) the interaction between bending moments acting along two orthogonal axes; 3) the stiffness and strength degradation in the cyclic behavior. In order to investigate the influence of these features, the following analyses are preformed:

1. Nonlinear static analysis of a symmetric structure;
2. Nonlinear static analysis of an asymmetric structure;
3. Nonlinear time history analysis of a symmetric structure;
4. Nonlinear time history analysis of an asymmetric structure.

The first analysis is carried out to assess the influence of the interaction between axial force and bending moment; the second analysis also includes the effect of the biaxial interaction. The third analysis is affected by the interaction between axial force – and bending moment and by the cyclic behavior; finally, all the features are involved when the nonlinear time history analysis of the asymmetric structure is considered.

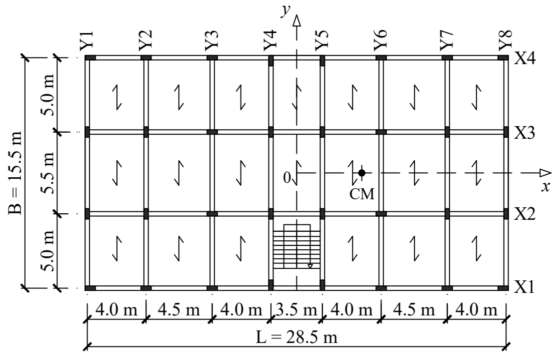

Fig. 1 – Plan layout of the building

3. Case Study

A five-story building with r.c. framed structure is considered in this study. The building is designed to resist gravity and seismic loads. The building is symmetric with respect to the *x*-axis (longitudinal direction) and experiences lateral-to-torsional coupling of the seismic response only for ground motions acting along the *y*-direction (transverse direction). The floor is rectangular in plan and has dimensions (*B* and *L*) equal to 15.5 m and 28.5 m (Fig. 1). The center of rigidity (CR) is coincident with the geometric center of the floor O. The centers of mass of the floors (CM) are lined up along a vertical axis. The position of this axis (Fig. 1) is shifted with respect to the center of rigidity so as to obtain a value of the rigidity eccentricity e_r equal to –0.15 *L*. The mass and the radius of gyration of the mass r_m (calculated with respect to the center of mass of the floor) are equal to 477.7 t and 9.87 m (0.346 *L*), respectively.

The floors are sustained by four seven-bay frames arranged along the *x*-axis (from X1 to X4) and by eight three-bay frames arranged along the *y*-axis (from Y1 to Y8). The characteristic value of the dead load is equal to 5.6 kN/m^2 for the floor and equal to 4.2 kN/m^2 for the staircase; the characteristic values of the live load of the floor and the staircase are 2.0 kN/m^2 and 4.0 kN/m^2, respectively. The characteristic value of the weight of the infill walls is 7.0 kN/m. Beams and columns are made of concrete C20/25 [4] (see Eurocode 2) with a characteristic compressive cylindrical strength f_{ck} = 20 MPa. Steel grade with a characteristic yield strength f_{yk} = 430 MPa is used for the longitudinal and transverse reinforcements. The building is designed according to the regulations in force in Italy from 1996 to 2008 [4], [5] . In the design phase, the seismic forces are applied to two separate planar models of the structure for the *x*- and *y*-directions. Further details are reported in [6].

4. Modelling of the buildings

The numerical analyses are carried out by means of the OpenSees program [7]. The building is represented by means of a 3D centerline model with rigid diaphragms. Beams and columns are modelled by means of elements (Beam With Hinges Elements) which are elastic in the middle part and inelastic at the ends within a length L_{pl} equal to the maximum dimension of the member cross-section. The torsion stiffness is neglected. Fiber cross-sections are considered within the inelastic region of the beam members. To avoid the axial force in beams modelled by fibers in the presence of rigid diaphragms, Zero Length Section elements are added at one end of each beam. These zero length elements have very low axial rigidity and very high shear and flexural rigidity. Given the high aspect ratio of the members, the contribution of shear deformability to the structural response is neglected. Two different solutions are adopted to simulate the cross-section behavior within the inelastic region of columns: 1) fiber cross-sections; 2) moment-curvature relationships.

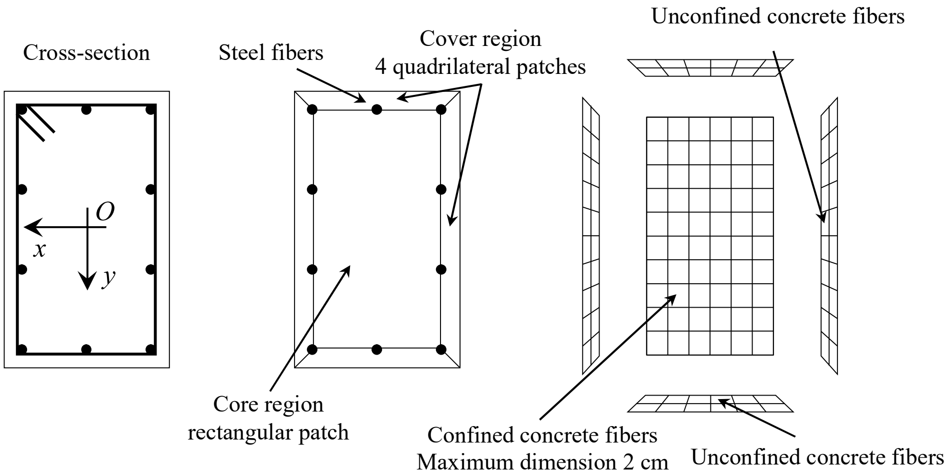

Fig. 2 – Fiber modeling of r.c. cross-section in Opensees

4.1 Fiber cross-sections

In the reference model (model F), the behavior of the plastic hinge is defined by assigning cross-sections discretized by means of fibers subjected to uniaxial stresses (Fig. 2). The maximum dimension of each fiber is 2 cm x 2 cm. The mechanical properties of the fibers are assigned so as to simulate the response of longitudinal reinforcement and concrete. To consider the effect of confinement on concrete, distinction is made between cross-section core (confined concrete) and cover (unconfined concrete). The response of the longitudinal steel bars is simulated by means of the Giuffrè-Menegotto-Pinto model [8], as modified by Filippou et al. [9] and implemented in OpenSees as "Steel02" uniaxial material. Referring to this model, note that the isotropic hardening is neglected in this study and that only the kinematic hardening is considered (the parameter b responsible for the kinematic hardening is assumed equal to 0.003). The uniaxial material model adopted for concrete is implemented in OpenSees as "Concrete04". If fibers are subjected to negative axial deformations (shortening), the monotonic response of this model is that proposed by Mander et al. [10]. Loading and unloading paths follow the rules proposed by Karsan and Jirsa [11], i.e. they are linear but their slope decreases with the increase in the uniaxial deformation. The response under positive axial deformations (elongation) is described by an initially linear function and by a nonlinear softening branch with a degradation exponential function. The loading and unloading paths are linear with slope equal to the secant stiffness at the point where the unloading path takes place.

The axial (compressive and tensile) strengths are equal to the mean values of the axial strengths of the assumed materials. The mean yield strength of the rebars f_{ym} is equal to 450 MPa. The mean compressive strength of unconfined concrete f_{cm} is equal to 28 MPa, while the mean tensile strength of concrete f_{ctm} is equal to 3.3 MPa. The ultimate axial deformation of the unconfined concrete ε_{cu} is assumed equal to 0.004. The compressive strength of confined concrete is evaluated as proposed by Mander et al. [10]. First, the values of the compressive strength and ultimate deformation of confined concrete are calculated for all the beams and columns; second, their average values are considered for the whole structure. In particular, the compressive strength of the confined concrete is assumed equal to 34 MPa. The ultimate deformation of confined concrete is assumed equal to 0.01.

4.2 Moment-curvature cross-sections

In the three simplified considered models, two independent moment–curvature relationships are assigned within the hinge region to simulate the nonlinear behavior along two orthogonal axes of the cross-section of the columns. The three models differ because of the adopted moment–curvature relationship. Specifically, two variants of bi-linear moment-curvature relationship are included in this investigation because they have been widely adopted in past studies with concentrated plasticity models; a multi-linear moment-curvature relationship is also considered to comment on the effect of the adoption of two independent hinges in the orthogonal directions when properly defined moment–curvature relationships are adopted.

To obtain the moment-curvature relationships, the deformation capacity of the columns is first determined in terms of chord rotation. In keeping with Eurocode 8 – Part 3 [12], the ultimate chord rotation θ_{um}, i.e. the chord rotation corresponding to the near collapse limit sate, is determined as:

$$\theta_{um} = \frac{1}{\gamma_{el}} 0.30^{\nu} \left[\frac{\max(0.01;\omega')}{\max(0.01;\omega)}\right]^{0.225} \left(\frac{L_V}{h}\right)^{0.35} 25^{\alpha\rho_{st}\frac{f_{yw}}{f_{cm}}} \tag{1}$$

where γ_{el} is equal to 1.5, h is the depth of the cross-section, ω and ω' are the mechanical reinforcement ratio of the tension and compression longitudinal reinforcements, respectively; ρ_{st} is the ratio of transverse reinforcement parallel to the direction of loading, α is the confinement effectiveness factor, f_{cm} and f_{yw} are the concrete compressive strength and the stirrup yield strength, L_V is the shear span at member end and ν is the ratio of the axial force N to the axial resistance of concrete bhf_{cm}. In this paper, the ultimate chord rotation is calculated with reference to the axial force N_G due to gravity loads in the seismic design situation and the shear span is calculated under the hypothesis that both the ends of the member develop the plastic moment reduced because of the axial force N_G.

Second, the moment-curvature analysis of the fiber cross-section subjected to the axial force produced by gravity loads is carried out up to an ultimate curvature equal to

$$\chi_{lim} = \frac{\theta_{um}}{L_{pl}} \tag{2}$$

Finally, for each orthogonal axis of the cross-section, the obtained moment-curvature curve is replaced by an idealized bi-linear curve (Model M1 and Model M2) or by a multi-linear curve (Model M3). The selection of a proper bi-linear curve to represent the moment-curvature relationship is a key issue. Different equivalence conditions have been suggested in the literature to define the bi-linear curve once the relevant range of interest of the curvature is defined. One possible approach (Model M1 in Fig. 3a) requires that the yield value of the bending moment M_{pl} be equal to the strength corresponding to the target curvature and that the curvature at yielding be chosen in such a way that the areas under the actual and the idealized curves be equal. This approach, which is widely adopted by engineers because of its simplicity, leads to a good estimate of the yield value of the

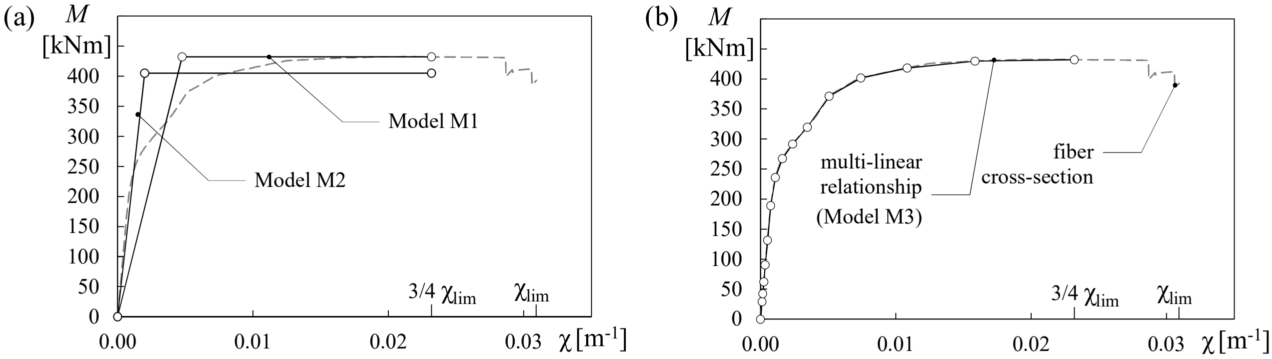

Fig. 3 – Idealized moment-curvature relationships: a) bi-linear; b) multi-linear

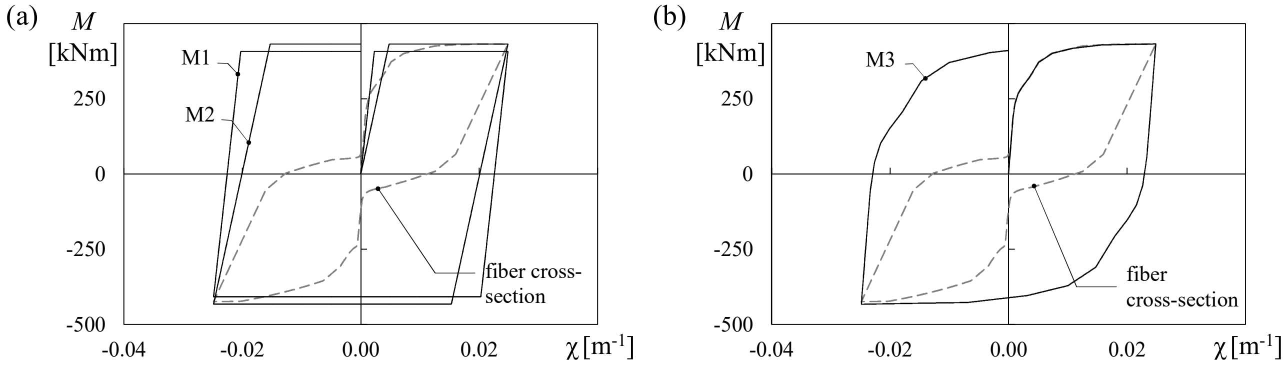

Fig. 4 – Simplified cyclic moment-curvature relationship vs actual behavior of the cross-section

bending moment but considers a reduced stiffness of the cross-section. A second approach requires that the bi-linear curve intercept the actual curve at a value of bending moment equal to 0.6 times the yielding value M_{pl} and that the areas under the actual and the idealized curves be equal. This approach leads to a bi-linear curve (shown as Model M2 in Fig. 3a) that underestimates the yield value of the bending moment but properly reproduces the elastic stiffness of the cross-section. Note also that, independently of the approach followed, the bi-linear curve depends on the relevant range of interest of the curvatures. In this paper, in order to reproduce the common practice, both the bi-linear curves previously described have been considered and the target curvature is assumed equal to $3/4\chi_{lim}$ (see Fig. 3a). This reference value (i.e. ¾ of the ultimate rotation) is adopted in Eurocode 8 – Part 3 as a reference value for the Significant Damage limit state. This value has been selected here to have moment-curvature relationships that provide an intermediate behavior. In the OpenSees model, the bi-linear curve is assigned to the cross-sections by the uniaxial material "Hardening".

When the multi-linear curve is used (model M3), numerical and idealized curves coincide in 15 points. These points are distributed between $\chi = 0$ and $\chi = 3/4\chi_{lim}$ according to a logarithmic distribution (see Fig. 3b). The figure shows that the multi-linear curve is able to model properly the monotonic rotational response of the cross-section under uniaxial bending (i.e. when there are not interaction phenomena). In the OpenSees model, the multi-linear curve is assigned to the cross-sections by the uniaxial material "multilinear".

Finally, Fig. 4 shows a comparison of the cyclic moment-curvature relationship obtained by analyzing a fiber cross-section (dashed line) and the corresponding cyclic responses predicted by the bi-linear and multi-linear models. The figure shows that, even when the monotonic moment-curvature relationship is properly described (i.e. when the multi-linear curve is used), the simplified model greatly overestimates the energy dissipated within the plastic hinge. Indeed, none of the adopted moment-curvature relationships is able to replicate the hysteretic degradation and the pinching, which are obtained when fiber cross-sections are used.

5. Eigenvalue analysis of the structure

As a preliminary step, the periods of vibration obtained for the asymmetric structure and those of the corresponding torsionally balanced structure (obtained by moving the centers of mass into the centers of rigidity) are determined by an eigenvalue analysis and the obtained values are listed in Tables 1 and 2. The eigenvalue analysis has been performed for each of the considered model. For each period, the directions involved in the

Table 1 – Periods of vibration of the asymmetric structure

Model	Mode 1	Mode 2	Mode 3	Mode 4	Mode 5	Mode 6
F	**0.716** (y-θ)	0.588 (x)	0.470 (θ-y)	**0.232** (y-θ)	0.193 (x)	0.153 (θ-y)
M1	1.016 (y-θ)	0.865 (x)	0.667 (θ-y)	0.357 (y-θ)	0.305 (x)	0.235 (θ-y)
M2	0.814 (y-θ)	0.685 (x)	0.534 (θ-y)	0.276 (y-θ)	0.235 (x)	0.181 (θ-y)
M3	0.715 (y-θ)	0.587 (x)	0.469 (θ-y)	0.232 (y-θ)	0.193 (x)	0.152 (θ-y)

Table 2 – Periods of vibration of the torsionally balanced structure

Model	Mode 1	Mode 2	Mode 3	Mode 4	Mode 5	Mode 6
F	**0.614** (y)	0.588 (x)	0.548 (θ)	**0.199** (y)	0.193 (x)	0.178 (θ)
M1	0.865 (x)	0.858 (y)	0.790 (θ)	0.305 (x)	0.302 (y)	0.277 (θ)
M2	0.694 (y)	0.685 (x)	0.627 (θ)	0.235 (y)	0.235 (x)	0.213 (θ)
M3	0.613 (y)	0.587 (x)	0.547 (θ)	0.199 (y)	0.193 (x)	0.178 (θ)

mode of vibration are also specified. The tables show that the adoption of bi-linear moment-curvature relationships defined according to the first approach (model M1) leads to an increase in the periods of vibration of about 50% for both the asymmetric and the torsionally balanced structures. The increase in the periods is limited to 17% when the model M2 is adopted. Finally, as expected, the model with multi-linear moment-curvature relationships properly reproduces the elastic properties of the structures.

6. Numerical Analyses

The seismic response of the considered building is evaluated by nonlinear static analysis and time-history analysis. The seismic response is determined along the y-direction. Further, the selected analysis is performed two times. The first time the analysis is carried out with reference to the asymmetric system; the second time, the same analysis is carried out for the corresponding planar system, i.e. for a system where the floor rotations and the displacements along the x-direction are restrained.

When nonlinear static analysis is performed, a set of horizontal forces is applied in the y-direction and distributed along the height according to an inverted triangular load pattern. The forces are applied to the centers of mass. The pushover analysis is stopped when the displacement of the center of mass of the top floor of the planar structure is equal to the displacement demand corresponding to an assigned PGA. In this paper, the PGA is set equal to 0.43 g and the displacement demand is determined by the N2 method [13].

When nonlinear time-history analysis is carried out, the seismic input is given by seven artificial bidirectional ground motions, compatible with the Eurocode 8 elastic spectrum for soil type C and characterized by 5% damping ratio and peak ground acceleration a_g equal to 0.35 g. The SIMQKE computer program is used to generate the accelerograms [14]. Each accelerogram is characterized by a total duration of 20 s and is enveloped by a "compound" function. The duration of the stationary part of the accelerogram is equal to 7.0 s and thus lower than the minimum value suggested in Eurocode 8, i.e. 10 s. The adopted value has resulted from a previous investigation in which natural and artificial accelerograms were compared in terms of the input energy spectra, Arias intensity, frequency content and number of equivalent cycles [15]. The mean of the peak ground accelerations of the generated accelerograms is not lower than the value stipulated in Eurocode 8 and no value of the mean response spectrum is lower than 90% of the corresponding value proposed in Eurocode 8.

The accelerograms are scaled to obtain a peak ground acceleration equal to 0.43 g. A Rayleigh viscous damping is used and set at 5% for two modes of vibration of the r.c. structures. The two selected modes are marked in bold type in Tables 1 and 2. The stiffness-proportional damping coefficient was applied to the tangent stiffness matrix of the elements. The equations of motion are integrated by means of the Newmark method with coefficients α=0.5 and β=0.25. The step of integration of the time-history is equal to 0.01 s. The algorithm used for the solution of the equilibrium equations is the Krylov-Newton algorithm. P-Δ effects are not considered in the analysis.

7. Comparison of the predicted responses

In this section, the seismic response predicted by the four considered models is compared.

7.1 Non linear static analysis

Fig. 5 shows the base shear vs the displacement of the center of mass of the top story (i.e. the pushover curve) predicted by the four considered models in the planar (Fig. 5a) and asymmetric (Fig. 5b) systems. When the planar structure is considered, the model with multi-linear moment-curvature relationships is able to reproduce properly the pushover curve obtained by the refined fiber model. Thus, the axial force-bending moment interaction does not affect the prediction of the response significantly. The models with bi-linear moment-

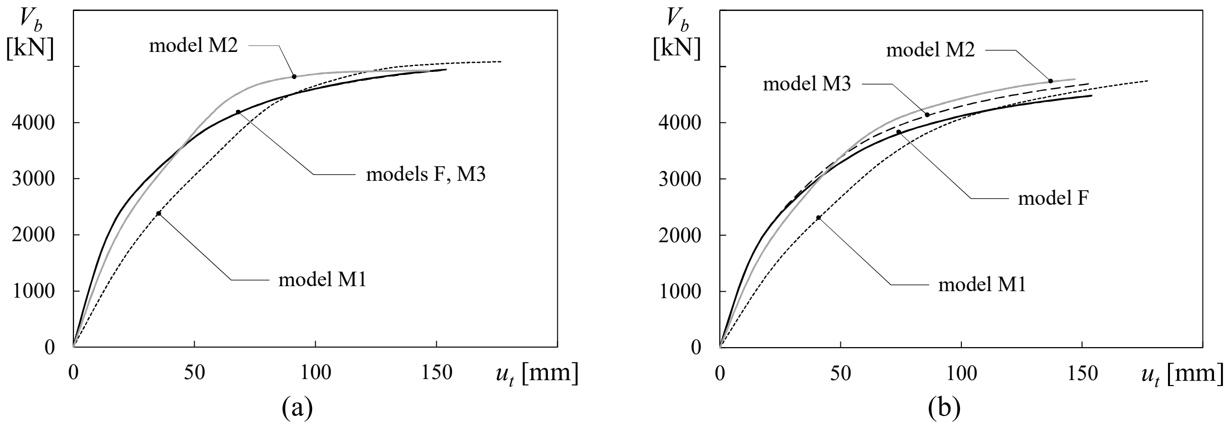

Fig. 5 – Pushover curves predicted by the models: a) planar structure; b) asymmetric structure

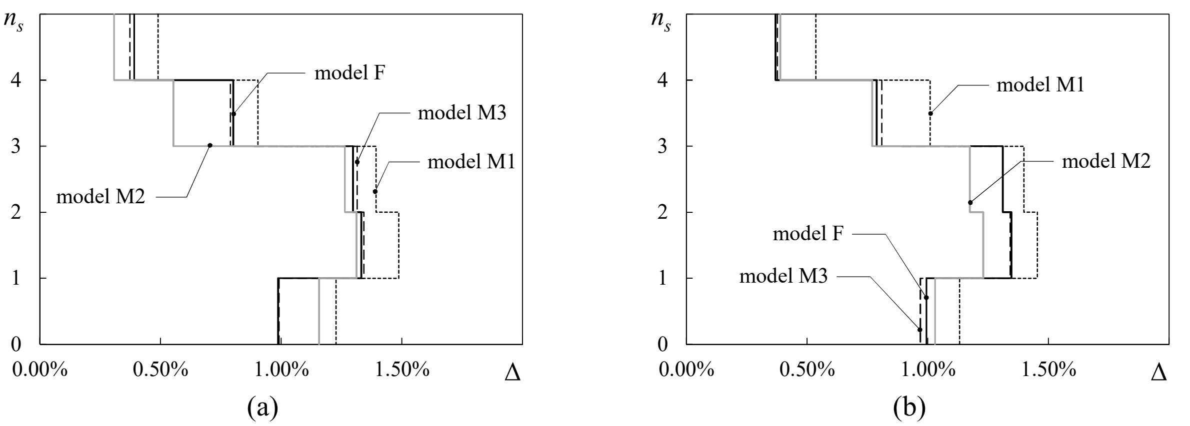

Fig. 6 – Story drifts corresponding to the top displacement demand: a) planar structure; b) asymmetric structure (values given at CM)

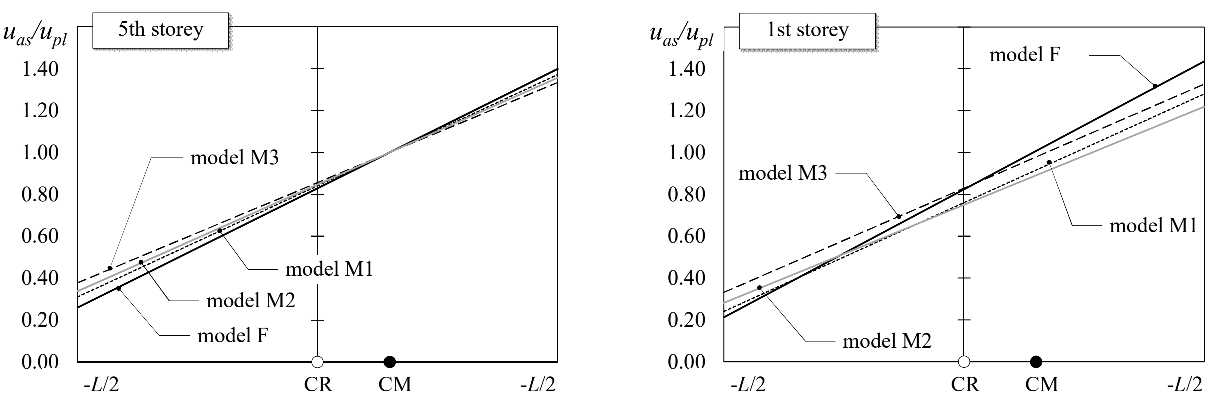

Fig. 7 – Torsional effects predicted by the models

curvature, instead, are more flexible. The lower stiffness also affects the prediction of the displacement demand given by the N2 method. Indeed, the top story displacement demand corresponding to a PGA equal to 0.43g is equal to 175 mm in model M1, and about to 150 mm in the other models.

Similar considerations apply to the asymmetric structure. However, in this case, the model with multi-linear moment-curvature relationships overestimates the ultimate base shear.

The distribution of story drifts corresponding to the above top displacement demand is shown in Fig. 6. Specifically, when the asymmetric structure is considered, the values of the drifts recorded at the center of mass are represented. The results shown in this figure are in keeping with those previously described, i.e. the drifts are larger when model M1 is adopted. However, the heightwise distribution of drifts is not extremely affected by the adopted model.

Finally, Fig. 7 shows the ratio of the displacements predicted in the asymmetric system (u_{as}) to the displacements of the corresponding planar system (u_{pl}) at the 5th and 1st story. The figure shows that the highest torsional effects are recorded when the model with fiber cross-section is used, while the lowest torsional effects are recorded when multi-linear moment-curvature relationships are adopted. Indeed, at the stiff side of the floor (x = -L/2), the reduction of displacements due to torsional effects is about 0.24 or 0.36 when the model F or M3 is adopted. Similarly, the increase of displacements at the flexible side ($x = L/2$) is 1.42 or 1.30 for models F and M3. Intermediate results are obtained for model M1 and M2.

7.2 Non linear time history analysis

In this section, the seismic responses determined by time history analysis with all the considered models are averaged over the number of accelerograms and compared. Fig. 8a shows the displacements obtained at each story of the planar frame. A continuous black line is used to simulate the response of model F, different dashed lines are used for models M1 and M3 while a grey line represents results of model M2. The displacements obtained in the model with cross-sections discretized by fibers are significantly higher than those obtained in the other models. As an example, at the top story, the displacement predicted by model F is about 200 mm, while that predicted by model M3 is lower than 150 mm. These differences are expected to be related to the stiffness and strength degradation and to pinching, which affect the cyclic behavior of fiber cross-sections only. Intermediate results are given by model M1 and M2. In particular, in model M1, the absence of pinching and degradation is partially counterbalanced by the higher deformability of the structure. Note also that displacements are underestimated by model M2 and M3 especially at the upper stories. The same considerations apply to the displacements of the center of mass of the asymmetric structure (Fig. 8b).

Finally, Fig. 9 shows, for each considered model, the ratio of the displacements of the asymmetric system to the

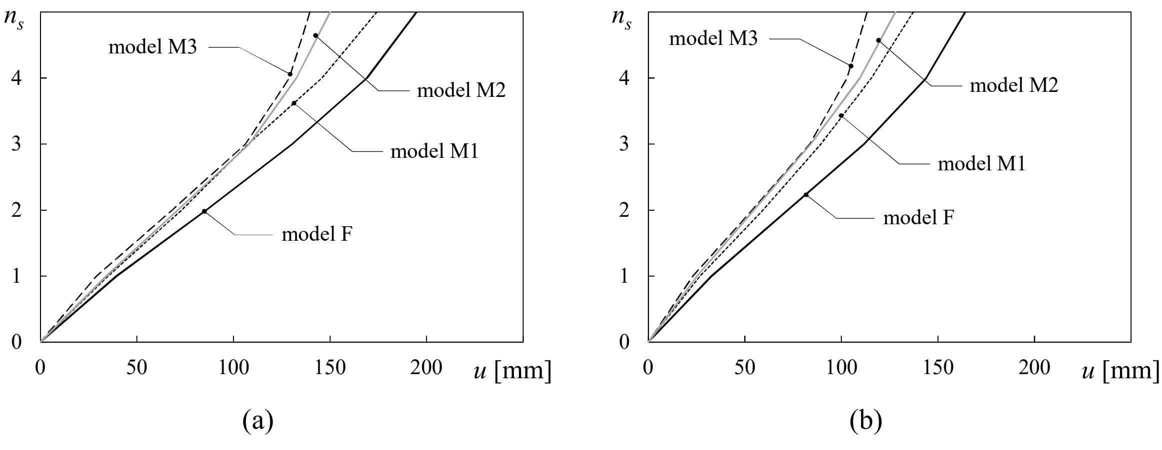

Fig. 8 – Floor displacements predicted by time-history analysis in the:
(a) planar structure; (b) asymmetric structure (values given at CM)

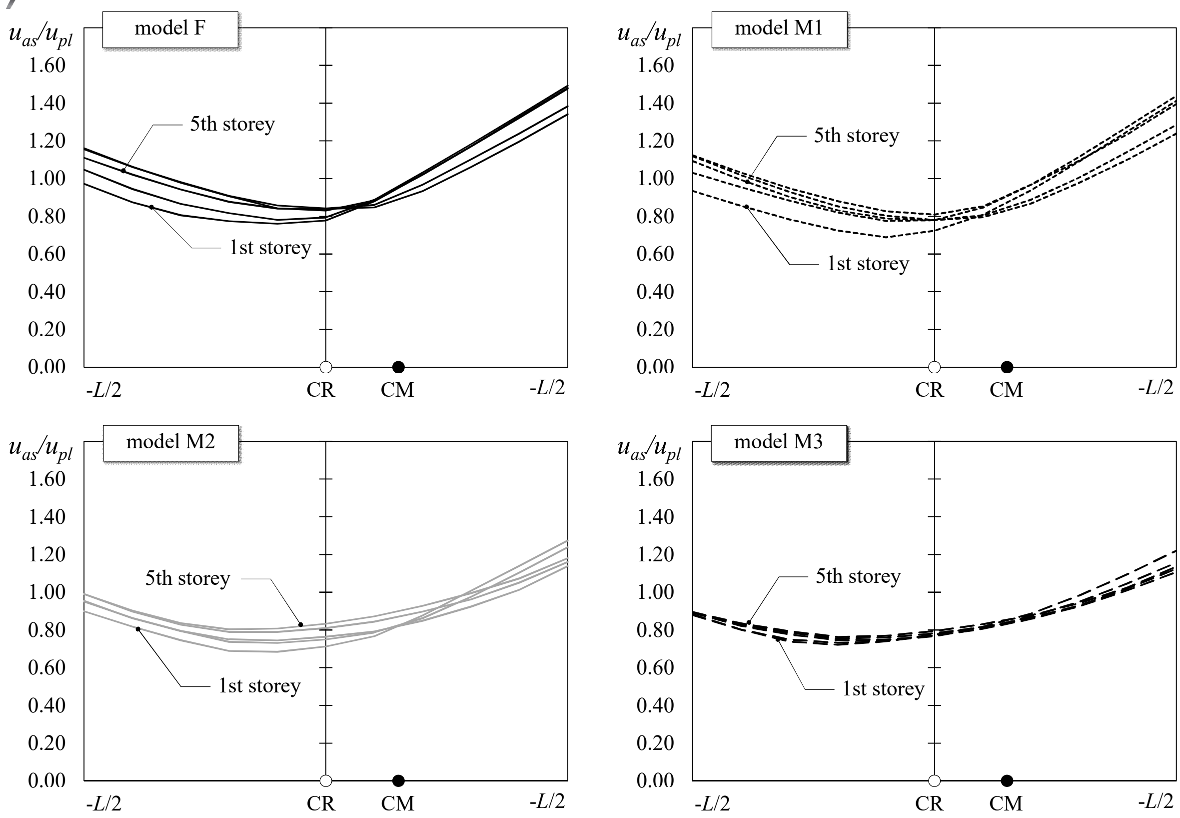

Fig. 9 – Torsional effects predicted by time-history analysis

corresponding displacements of the planar system (u_{as}/u_{pl}). Five lines are plotted in each figure to represent the response of each floor. The figure shows that the differences between the rotational responses predicted by the models are lower than the corresponding differences predicted when the nonlinear static analysis is performed (Fig. 7). This result is in keeping with the finding of a previous study on the seismic behavior of single story asymmetric structures sustained by either uni-axial resisting elements or bi-axial resisting elements [16]. Out of the considered models with moment-curvature relationship, model M1 gives the best estimate of the torsional response. Indeed, at the stiff side, the variation in the dynamic displacements due to torsional effects is in the range 1.00 – 1.16 according to the reference model F, 0.95 – 1.12 according to model M1. Similarly, at the flexible side the ratio u_{as}/u_{pl} is in the range 1.34 – 1.49 for model F, in the range 1.24 – 1.44 for model M1.

The highest differences in the prediction of the torsional response are obtained when model M3 is used. In fact, the model with multi-linear moment-curvature relationships predicts a reduction of the displacements due to torsional effects (u_{as}/u_{pl} equal to 0.9) at the stiff side and a slight increase of the displacements (u_{as}/u_{pl} lower than 1.2) at the flexible side. Further, the figure shows that the curves representing the different stories are less scattered when the model with multi-linear moment-curvature relationships is used. Note that, in the elastic range of behavior, the curves representing u_{as}/u_{pl} at each story are equal in a regularly asymmetric system.

8. Conclusions

The paper investigates the influence of modelling in the evaluation of the seismic response of asymmetric buildings. In particular, four models are compared. The models differ because of the cross-sections assigned within the hinge region of force Beam-Column elements. In the reference model, fiber cross-sections are assigned. In the other models, two independent moment–curvature relationships are assigned to simulate the nonlinear behavior along two orthogonal axes of the cross-section. In particular the considered relationships are:

- multi-linear moment-curvature relationships;

– bi-linear moment-curvature relationships characterized by a yield value of the bending moment equal to the strength corresponding to the target curvature;
– bi-linear moment-curvature relationships that intercept the actual curve at a value of bending moment equal to 0.6 times the yielding value.

Based on the comparison of the response predicted by the simplified models and that predicted by the reference model, the following conclusions are drawn

– The model with multi-linear moment–curvature relationships can accurately predict the non-linear static response of a symmetric structure.
– Models with two independent moment–curvature relationships significantly underestimate the torsional effects in asymmetric structures when non-linear static analysis is performed.
– Models with two independent moment–curvature relationships significantly underestimate the floor displacements of both the symmetric and asymmetric structures when non-linear dynamic analysis is performed.
– Out of the considered simplified models, the one with bi-linear moment-curvature relationships characterized by a yield value of the bending moment equal to the strength corresponding to the target curvature gives the best prediction of the dynamic response. Indeed, the higher deformability that characterized the structure when this model is used partially counterbalances the effects of stiffness and strength degradation.
– The differences in the rotational response predicted by the considered models when the dynamic analysis is performed are lower than those predicted when the nonlinear static analysis is carried out.

Note that the conclusions above are based on the results of a single case-study. Further analyses are required to generalize the results of this study. Further, the effectiveness of a model with two independent moment–curvature relationships able to reproduce stiffness and strength degradation needs to be investigated.

9. Acknowledgements

The authors gratefully acknowledge funding provided by the (Italian) Department of Civil Protection (project DPC-ReLUIS 2010/2013 Task 1.1.2. "Strutture in cemento armato ordinarie e prefabbricate"). The opinions expressed in this paper are those of the writers and do not necessarily reflect the views of the sponsors.

10. References

[1] Clough RW, Benuska KL, Wilson EL (1965): Inelastic earthquake response of tall buildings. *3rd World Conference on Earthquake Engineering*, Wellington, New Zealand.

[2] Giberson MF (1967): The response of nonlinear multistory structures subjected to earthquake excitation. PhD thesis, California Institute of Technology, Pasadena, Calif.

[3] Scott MH, Fenves GL (2006): Plastic Hinge Integration Methods for Force-Based Beam–Column Elements. *Journal of Structural Engineering*, ASCE, **132**(2), 244-252.

[4] CEN. Eurocode 2: Design of concrete structures. Part 1-1: General rules and rules for buildings, EN 1992–1. European Committee for Standardization: Bruxelles, Belgium, 1992.

[5] Italian Ministry of Public Works: Ministry Decree, 16/01/1996, Norme tecniche per le costruzioni in zone sismiche (Regulations for constructions in seismic areas), *Gazzetta Ufficiale Serie generale*, 5/02/1996, Rome. (in Italian)

[6] Bosco M, Ferrara GAF, Ghersi A, Marino EM, Rossi PP (2015): Predicting displacement demand of multi-storey asymmetric buildings by nonlinear static analysis and corrective eccentricities. *Engineering Structures*, 99, 373-387.

[7] Mazzoni S, McKenna F, Scot MH, Fenves GL et al. (2007): OpenSees Command Language Manual.

[8] Menegotto M, Pinto PE. (1973): Method of analysis for cyclically loaded RC plane frames including changes in geometry and nonelastic behaviour of elements under combined normal force and bending. *IABSE Symposium*, Lisboa, Portugal.

[9] Filippou FC, Popov EP, Bertero VV (1983): Effects of bond deterioration on hysteretic behavior of reinforced concrete joints. Report UCB/EERC 83/19, College of Engineering, University of California at Berkeley.

[10] Mander JB, Priestley JN, Park R (1988): Theoretical stress-strain model for confined concrete. *Journal of Structural Engineering*, ASCE, **114**(8), 1804–1826.

[11] Karsan ID, Jirsa JO (1969): Behavior of concrete under compressive loading. *Journal of Structural Division*, ASCE, **95**(ST12).

[12] CEN. Eurocode 8 (2005): Design of structures for earthquake resistance - Part 3: Assessment and retrofitting of buildings, EN 1998–3. European Committee for Standardization: Bruxelles, Belgium.

[13] Fajfar P, Gaspersic P (1996): The N2 method for the seismic damage analysis of rc buildings. *Earthquake Engineering and Structural Dynamics*, **25**, 31–46.

[14] SIMQKE (1976): A program for artificial motion generation, User's manual and documentation, Department of Civil Engineering MIT.

[15] Amara F, Bosco M, Marino EM, Rossi PP (2014): An Accurate Strength Amplification Factor for the Design of SDOF Systems with P-Δ Effects. *Earthquake Engineering and Structural Dynamics*, **43**, 589–611.

[16] Bosco M, Ghersi A, Marino EM, Rossi PP (2016): Influence of the interaction yield domain on lateral-torsional coupling of asymmetric single-storey systems. Chapter 18 of the book Seismic Behaviour and Design of Irregular and Complex Civil Structures II, Z. Zembaty, M. De Stefano (eds.). *Geotechnical, Geological and Earthquake Engineering*, **40**, 205-214.